

Spectroscopy of Cobalt–Ethylenediamine–Oxygen Adducts in the Supercages of Zeolites †

By Robert A. Schoonheydt* and Jozefien Pelgrims, Centrum voor Oppervlaktischeikunde en Colloïdale Scheikunde, De Croylaan, 42, B-3030 Leuven (Heverlee), Belgium

The complex $[\text{Co}(\text{en})_3]^{2+}$ (en = ethylenediamine) can be synthesized in the supercages of faujasite-type zeolites by adsorption of gaseous en. On dehydrated cobalt-zeolites additional heating is necessary to enhance the mobility of Co^{2+} from the small cages to the supercages. Upon heating, $[\text{Co}(\text{en})_3]^{2+}$ decomposes to $[\text{Co}(\text{en})_2]^{2+}$ and to $[\text{Co}(\text{en})]^{2+}$. The mono and tris complexes are not capable of binding O_2 whereas the bis complex forms the 1 : 1 superoxo-complex $[\text{Co}(\text{en})_2(\text{O}_2)]^{2+}$ and the 2 : 1 monobridged peroxo-complex $[\{\text{Co}(\text{en})_2\}_2(\text{O}_2)]^{4+}$ with O_2 . The former is preferentially formed when not more than one cobalt atom is in each supercage, the latter when more than one cobalt, statistically, is in each supercage. The 1 : 1 superoxo-complex is unstable, and its formation is only partially reversible. The amount of electron transfer from cobalt to O_2 is estimated to be 0.46 e, indicating a weak σ -donor ligand *trans* to O_2^- in the complex. When $[\text{Co}(\text{en})_3]^{2+}$ and physisorbed en are present in the supercages the interaction with O_2 is complex and involves oxidation of en with formation of water.

MONONUCLEAR superoxo-complexes of cobalt are well known in inorganic chemistry. The main method for their characterization, until now, was e.s.r. The use of bulky unsaturated ligands with strong u.v. absorptions prevented a complete study of the *d-d* and charge-transfer transitions of these systems. Recently, however, this difficulty was overcome with the isolation of chlorobis(*NN'*-dimethylethylenediamine)superoxo-cobalt(III) and a consistent interpretation of the spectra of mono- and di-nuclear superoxo- and peroxo-cobalt complexes is now available.¹⁻⁵

Mononuclear and dinuclear superoxo-complexes can also be synthesized in the supercages of faujasite-type zeolites with u.v.-transparent ligands such as NH_3 , mono-alkylamines, and ethylenediamine (en).^{6,7}

The supercages of the zeolites X and Y offer several advantages for the isolation of mononuclear superoxo-complexes over regular solutions. First, the complexes are immobilized on the surface and dimerization processes are strongly retarded. Secondly, the negatively charged surface can act as a solvent, a ligand, or an anion to stabilize the complexes. Thirdly, the surface-stabilized complexes offer new methods for controlled oxidation reactions. The potential use of the mononuclear superoxo-complex of cobalt and en in the supercages of zeolites Y has been demonstrated by Lunsford and co-workers both for a biologically important reaction, the oxidation of pyrocatechol,⁸ and for the oxidative dehydrogenation of cyclohexa-1,4-diene to benzene.⁹

Up to now, superoxocobalt complexes in zeolites have only been studied by e.s.r. and i.r. spectroscopy.^{6,7,9} It is clear now that not all the cobalt ions were converted to the mononuclear superoxo-form and that the ligand en was attacked by O_2 .^{7,9} We introduce the technique of reflectance spectroscopy not only to allow a complete spectroscopic study of the mononuclear superoxo-complex itself but also to identify the complexes before and after the interaction with O_2 and to study the reversibility of superoxo-complex formation.

† This work was presented in part at the Sixth North American Meeting of the Catalysis Society, Chicago, 12–17 March, 1979.

EXPERIMENTAL

Sample Preparation.—Synthetic Y-type zeolites without binder from Union Carbide's Linde Division were stirred in 1 mol dm^{-3} NaCl solutions at room temperature, washed to free them from chloride ion, air-dried, and stored over a saturated $[\text{NH}_4]\text{Cl}$ solution prior to use. Cobalt zeolites with a variable cobalt content were prepared by exchange of NaY (10⁻³ kg) in solution (1 dm^3) with sufficient Co^{2+} to obtain the desired exchange level at room temperature for 8.64×10^4 s. Maximum exchange levels were obtained with the same procedure but the Co^{2+} concentration in the exchange solution was 0.0033 mol dm^{-3} . A sample of Co-LaY was prepared by first exchanging NaY in $\text{La}[\text{NO}_3]_3$ (0.0033 mol dm^{-3}) at room temperature with a solid : liquid ratio of 1 g dm^{-3} during 8.64×10^4 s. The LaY was then washed anion-free, air-dried, and calcined in a crucible in a muffle furnace at 823 K during 8.64×10^4 s. The subsequent Co^{2+} exchange was performed as described above for maximum yield. In another preparation NaY was converted to KY at 353 K prior to Co^{2+} exchange. All the samples were washed anion-free, air-dried, and stored over a saturated $[\text{NH}_4]\text{Cl}$ solution in a desiccator. The ions Na^+ , K^+ , and Co^{2+} were determined by atomic absorption spectrometry after $\text{HF-H}_2\text{SO}_4$ dissolution of the minerals. For La^{3+} the emission line at 441.7 nm was used. Table I summarizes these analytical data. The sample abbreviations used comprise the symbols of the exchangeable cations other than Na^+ , the type of zeolite, and the number of Co^{2+} ions per unit cell in parentheses.

Procedures.—Two types of experiments were performed, aimed respectively at (i) the formation and thermal de-

TABLE I

Exchangeable cation content (mequiv. g^{-1}) of the zeolites

Sample	Co^{2+}	La^{3+}	Na^+	K^+
CoY(1.6)	0.25		3.89	
CoY(5.3)	0.80		3.33	
CoY(7.1)	1.10		3.21	
CoKY(7.2)	1.12		0.71	2.19
CoY(8.1)	1.27		3.38	
CoY(11.0)	1.72		2.36	
CoY(12.2)	1.90		2.16	
CoY(17.0)	2.65		1.68	
CoY(18.0)	2.73		1.41	
CoLaY(5.8)	0.91	2.27	1.05	
CoA(1.3)	1.65		5.86	
CoX(19.5)	2.85		3.32	

composition of Co^{2+} -en complexes, and (ii) the interaction of these complexes with O_2 , including a study of the reversibility of this reaction.

Formation and thermal decomposition of $[\text{Co}(\text{en})_3]^{2+}$
Cobalt zeolites (2–3 g) were loaded in a reflectance cell,¹⁰ while ca. 100 mg of the same zeolite were transferred to an aluminium foil sample holder, hooked onto a quartz spring balance (sensitivity: 0.5 mg mm^{-1}). Both the reflectance cell and the McBain balance were connected to the same vacuum line. The samples were dehydrated *in vacuo* ($< 1.35 \times 10^{-2} \text{ Pa}$) at various temperatures between room temperature and 723 K. The evacuation time varied from 3 600 to $1.728 \times 10^5 \text{ s}$ but in any case the weight loss was registered. The samples were cooled to room temperature and en, pre-dried over metallic Na, was allowed to adsorb from the gas phase. The adsorption was quantitatively followed on the McBain balance, while the changes in the co-ordination of Co^{2+} were recorded by reflectance spectroscopy. After saturation the samples were evacuated from room temperature up to 550 K in steps of 50 K. After each step the weight loss and the spectral changes were registered.

The interaction with O_2 . Oxygen ($6.67 \times 10^3 \text{ Pa}$) pre-purified in a zeolite A trap at liquid air temperature was allowed to adsorb at room temperature onto the samples obtained after decomposition of the cobalt(II) complexes in the range 415–550 K. The weight changes were registered continuously as a function of time.

A second series of experiments was conducted on similarly pretreated samples in order to investigate the reversibility of the interaction with O_2 . Thus, the reflectance spectra were recorded immediately after admission of O_2 and after room-temperature evacuation. Then, O_2 ($6.67 \times 10^3 \text{ Pa}$) was adsorbed for $1.08 \times 10^4 \text{ s}$ and the spectra recorded before and after room-temperature evacuation of O_2 . In a third step, the O_2 adsorption time was $8.64 \times 10^5 \text{ s}$. All the spectra were recorded in the range 210–700 nm with hydrated NaY as a standard, but special attention was also given to the 1 800–2 000 nm range to detect H_2O . These reversibility experiments were repeated on CoY(5.3) in a cell which allows one to record both reflectance and e.s.r. spectra. In these experiments, the decomposition temperature of the cobalt(II) complexes, prior to admission of O_2 , was held in the range 473–505 K.

Instrumental Techniques.—Reflectance spectra were recorded on a Cary 17 spectrometer with a type I reflectance unit and a $\text{Ba}[\text{SO}_4]$ reference. Full-length spectra (2 000–210 nm) were tape recorded, computer processed, and plotted as $F(R_\infty)$ or $\log[F(R_\infty)]$ against wavenumber after subtraction of the baseline. The baseline was recorded with two $\text{Ba}[\text{SO}_4]$ -filled reflectance cells; $F(R_\infty)$ is the Kubelka-Munk function relating R_∞ , the ratio of light intensity reflected from the sample to the light intensity reflected from the $\text{Ba}[\text{SO}_4]$ reference, to the apparent absorption coefficient and the apparent scattering coefficient of the material.¹¹

Spectra in the visible and u.v. regions only (210–700 nm) were recorded against the hydrated sodium form of the zeolite and plotted as such. Electron spin resonance spectra of the O_2^- complexes were recorded at 78 K in X-band on a Varian E-4 apparatus with a rectangular cavity. The g values were determined relative to diphenylpicrylhydrazyl (dpph) ($g = 2.0036$). In some cases an E-9 apparatus was used with a dual rectangular cavity and a Varian pitch ($g = 2.0028$) to determine g values.

RESULTS

The Formation and Decomposition of $[\text{Co}(\text{en})_3]^{2+}$ in the Supercages.—The room-temperature adsorption of en depends on the type of zeolite and its pretreatment. This is illustrated in Figure 1. Thus, on CoX and CoY, an in-

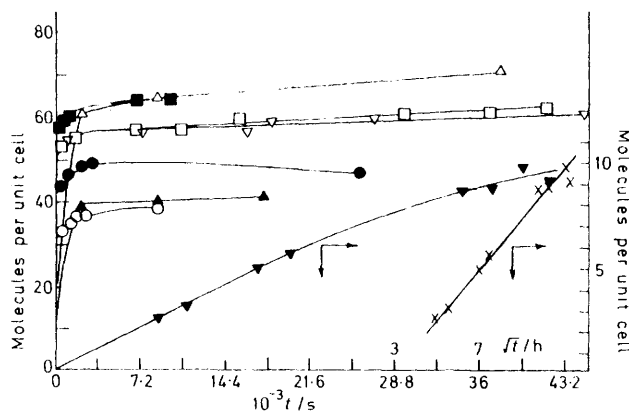


FIGURE 1 Room-temperature adsorption of ethylenediamine on Co^{2+} -zeolites as a function of time: CoY(12.2) pretreated at 673 K for $3.6 \times 10^3 \text{ s}$ (Δ); CoY(18) at 673 K overnight (\blacksquare); CoY(18) at room temperature overnight (\bullet); CoLaY(5.8) at 723 K overnight (\square); CoY(8.1) at 742 K overnight (∇); CoY(1.6) at 373 K overnight (\blacktriangle); CoA(1.3) at 673 K overnight (∇), *idem* but plotted against square root of time (\times). The right-hand vertical axis refers to plots ∇ and \times .

stantaneous adsorption step, giving ca. 90% saturation in the first hour, is followed by an extremely slow saturation. The latter can only be evidenced when the experiment is conducted over a period of several days. The presence of residual water reduces the adsorption capacity. For CoA(1.3) the initial, instantaneous adsorption step is missing. When the data points for CoA(1.3) are plotted against the square root of the time of adsorption a straight line is obtained, indicative of a diffusion-limited process.

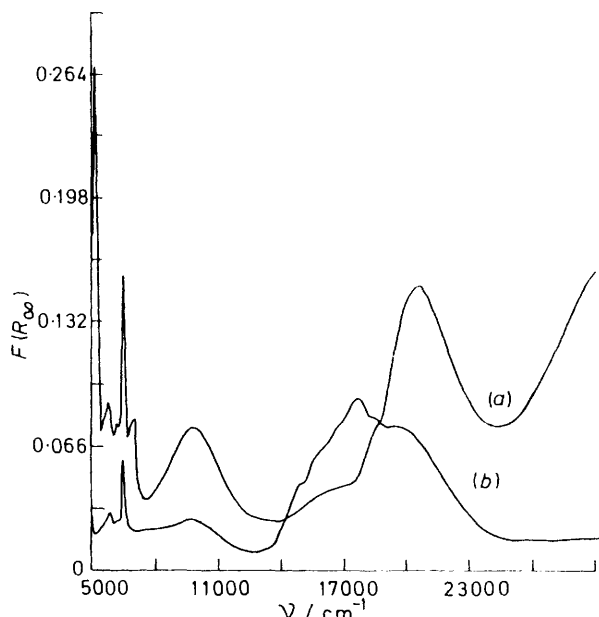


FIGURE 2 Reflectance spectra of en-saturated Co-zeolites. (a) CoY(5.3), evacuated at room temperature for $7.2 \times 10^3 \text{ s}$; (b) CoY(8.1), evacuated at 673 K

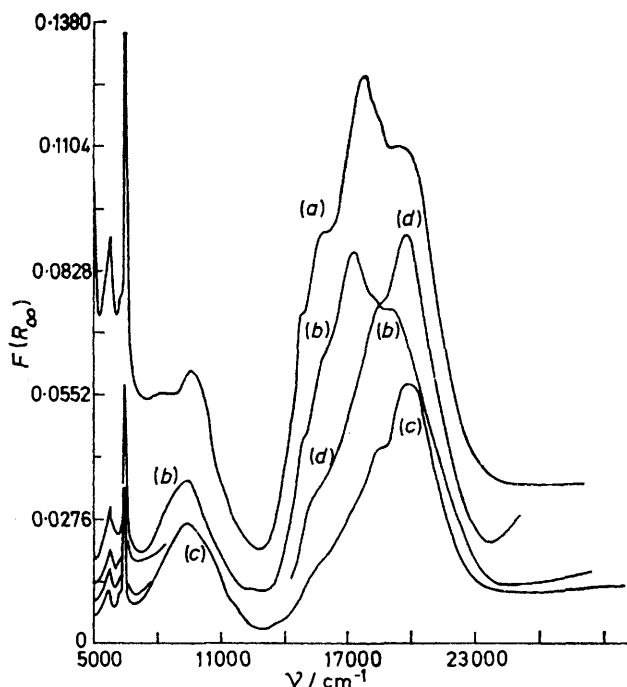


FIGURE 3 Reflectance spectra of CoY(8.1) pretreated at 723 K. (a) Saturated with en at room temperature; (b) evacuation at 329 K; (c) evacuation at 428 K; (d) evacuation at 477 K

Upon exposure to gaseous en, complete conversion of Co^{2+} to $[\text{Co}(\text{en})_3]^{2+}$ is only possible on hydrated zeolites, *i.e.* when all the Co^{2+} is present as $[\text{Co}(\text{OH}_2)_6]^{2+}$ in the supercages. The corresponding spectrum, shown in Figure 2, shows the typical $d-d$ transitions of $[\text{Co}(\text{en})_3]^{2+}$ at 10 000 cm^{-1} and 20 650 cm^{-1} , the latter with a shoulder at 18 400 cm^{-1} .¹² The spectrum also shows, in the near-i.r. region, the CH (5 600 cm^{-1}) and NH (6 500 cm^{-1}) vibrational overtones of en and the $\nu + \delta$ and 2ν vibrations of H_2O , at 5 220 and 7 000 cm^{-1} respectively. On dehydrated cobalt(II) zeolites, the saturation with en leads to a decrease in the $d-d$ band intensities of Co^{2+} co-ordinated to lattice oxygens and the appearance of the $[\text{Co}(\text{en})_3]^{2+}$ bands around 10 000 and 20 000 cm^{-1} (Figure 2). Complexation is incomplete even after prolonged exposure to en. In the visible region, bands of dehydrated Co^{2+} are located around 14 700, 15 700, and 17 600 cm^{-1} . The decrease in intensity of the first band can be used as a qualitative measure of the amount of $[\text{Co}(\text{en})_3]^{2+}$ formed after room-temperature saturation of dehydrated zeolites. The assumptions are that the scattering coefficient remains constant and that all the uncomplexed cobalt(II) ions contribute to the intensity of the band at 14 700 cm^{-1} before and after admission of en. The results, reported in Table 2, reflect the expected trend. Thus, at low cobalt concentrations, when nearly all the Co^{2+} ions are in the small cavities, most of them remain uncomplexed.¹³ The production of $[\text{Co}(\text{en})_3]^{2+}$ can be

TABLE 2

Estimated numbers of $[\text{Co}(\text{en})_3]^{2+}$ and Co^{2+} ions per unit cell after saturation

Sample	$[\text{Co}(\text{en})_3]^{2+}$	Co^{2+}	% Complexed
CoY(1.6)	0.3	1.3	19
CoY(12.2)	7.2	5.0	59
CoLaY(5.8)	4.1	1.7	71
CoX(19.5)	11.9	7.6	61

enhanced by blocking the sites in the small cages with La^{3+} ions.

Complete conversion of the residual dehydrated cobalt(II) species to $[\text{Co}(\text{en})_3]^{2+}$ can be achieved by slow heating *in vacuo*. Figure 3 demonstrates the progressive decrease in intensity of the bands due to dehydrated CoY(8.1) and the increase in intensity of the $[\text{Co}(\text{en})_3]^{2+}$ bands. After evacuation at 477 K nearly all cobalt(II) ions are converted to $[\text{Co}(\text{en})_3]^{2+}$. We note that in the absence of water, the bands of the tris complex are at 9 500 and 19 940 cm^{-1} , as compared to 10 000 and 20 650 cm^{-1} in the hydrated zeolite. In the latter case the removal of H_2O at 373 K leads to a broadening of the 10 000 cm^{-1} band and a red shift of its maximum, towards 8 500–9 000 cm^{-1} . The 20 640 cm^{-1} band is shifted towards 19 800 cm^{-1} and shoulders become visible at 18 100 cm^{-1} and 22 000 cm^{-1} . The conversion of Co^{2+} to $[\text{Co}(\text{en})_3]^{2+}$ upon heating masks these effects for dehydrated zeolites below *ca.* 423 K. However, Figure 4 clearly shows the red shift of the 9 500 cm^{-1} band and the appearance of the 22 000 cm^{-1} shoulder. Above 473 K the features of a pseudo-tetrahedral cobalt(II) complex appear. It becomes the dominant species after evacuation at 523 and 548 K. The spectrum of this pseudo-tetrahedral cobalt(II) ion consists of three groups of three bands in the near-i.r. region (5 900, 7 300, and 8 200 cm^{-1}), in the visible region (16 300, 17 500, and 18 700 cm^{-1}), and in the u.v. (28 400, 32 600, and 36 600 cm^{-1}) respectively.

The residual en contents of the zeolites after the various treatments are summarized in Table 3. It is shown that in all cases, except at the highest cobalt(II) loadings, the en : Co^{2+} ratio is $\geq 3 : 1$. Further, for identical desorption temperatures, the residual en content is roughly proportional to the cobalt(II) loading.

The Formation of Oxygen Adducts.—It was extremely difficult to obtain meaningful gravimetric results for a series of experiments on the same McBain balance. This was due to adsorption of en on the glass walls and extensive heating of the empty balance between two successive experiments

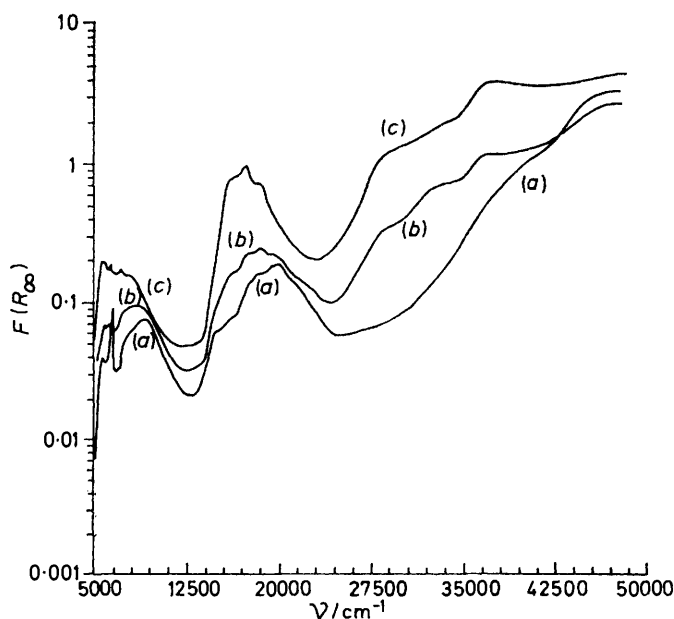


FIGURE 4 Reflectance spectra of the decomposition of $[\text{Co}(\text{en})_3]^{2+}$ on CoY(18). (a) Evacuated at 448 K; (b) evacuated at 498 K; (c) evacuated at 523 K

TABLE 3
Residual ethylenediamine contents

Sample	Desorption temperature/K	en/mols per unit cell
CoY(1.6)	473	25.4
CoY(8.1)	473	37.9
CoY(11)	473	37.8
CoY(12.2)	473	38.9
CoLaY(5.8)	473	33.3
CoX(19.5)	473	51.3
CoA(1.3)	473	4.25
CoY(5.3)	423	33.7
CoY(5.3)	458	26.2
CoY(5.3)	475	23.9
CoY(5.3)	498	19.0
CoY(17)	425	45.0
CoY(17)	448	35.7
CoY(17)	475	34.1
CoY(17)	525	20.4

was necessary to obtain reliable data. Figure 5 shows the time dependence of the O₂ adsorption process. There are two adsorption processes superposed on each other: an instantaneous step and a slow step stretching out over a period of several hours. The instantaneous adsorption

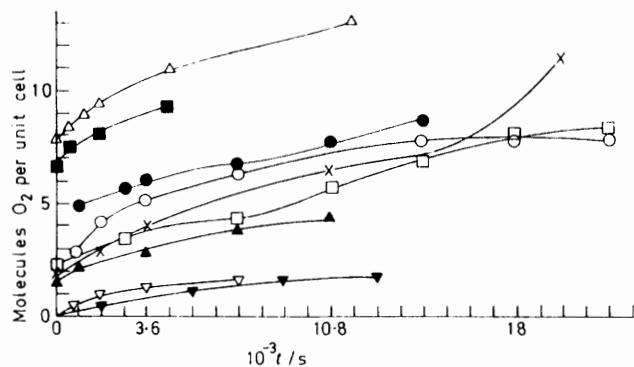


FIGURE 5 Room-temperature adsorption of O₂ (6.67×10^3 Pa) as a function of time: CoY(5.3), decomposition temperature of [Co(en)₃]²⁺ = 458 K (Δ); CoY(5.3), 475 K (\blacksquare); CoY(5.3), 498 K (\times); CoY(18), 444 K (\bullet); CoY(18), 418 K (\circ); CoY(18), 476 K (\square); CoY(18), 495 K (\blacktriangle); CoY(18), 547 K (∇); CoY(18), evacuated at room temperature (\blacktriangledown)

process is not present after evacuation of excess of en at 523 K and 548 K. In the latter cases O₂ does not provoke colour changes. When O₂ is adsorbed instantaneously the samples immediately assume a tan colour. Table 4 shows that the amount of instantaneously adsorbed O₂ is not only dependent on the cobalt content and the en:Co ratio but also on the pretreatment. Thus, after a low-temperature evacuation, prior to adsorption of en, cobalt(II) ions are mainly in the supercages, remain there in the presence of en, and are susceptible to interaction with O₂. At high en:Co ratios (or low cobalt content) an excess of uncoordinated en is present which may be oxidized by O₂.

In the reflectance spectra of the samples pretreated in the range 410–550 K, the cobalt(II) spectral features disappear upon admission of O₂ except those of lattice co-ordinated Co²⁺ and those of the pseudo-tetrahedral cobalt(II)–en species. This indicates that these species do not interact with O₂. In these cases there is also no instantaneous O₂ adsorption and no tan colouration. Thus, the occurrence of the latter two phenomena can be taken as qualitative evidence for the direct interaction of O₂ with [Co(en)_x]²⁺

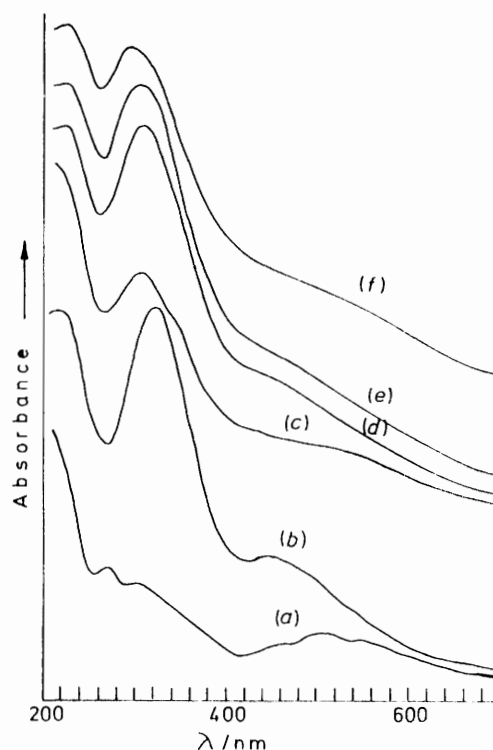


FIGURE 6 Reflectance spectra of the O₂ adducts of CoY(7.1) after evacuation at 673 K and saturation with en. (a) Degassed at 499 K; (b) immediately after admission of O₂ (6.67×10^3 Pa) at room temperature; (c) after evacuation of excess of O₂ overnight at room temperature; (d) after 1.08×10^4 s contact with O₂ (6.67×10^3 Pa) at room temperature; (e) after evacuation of O₂ at room temperature during 7.2×10^3 s followed by 7.2×10^4 s contact with O₂ (6.67×10^3 Pa) at room temperature; (f) after room-temperature evacuation of O₂ at room temperature for 14.4×10^3 s

with $x = 2$ or 3. At least two O₂ adducts are then formed, depending on the cobalt(II) content and the desorption temperature of en.

The sample CoY(7.1) interacts in two distinct ways with O₂ depending on the decomposition temperature of the en-saturated samples. After decomposition in the range 488–505 K the spectra of Figure 6 are produced. Thus, immediately after admission of O₂ (6.67×10^3 Pa) an intense band is produced at 320 nm with weaker features at 450 nm and around 500 nm. On the u.v. tail of the spectrum a shoulder at 230 nm is also visible. The 320 and 450 nm bands have to be interpreted, respectively, as the O₂⁻→Co^{III} and the Co^{III}→O₂⁻ charge-transfer transitions of the mononuclear superoxo-complex [Co^{III}(en)₂(O₂)²⁺]. The positions of these band maxima and their intensities agree with the

TABLE 4

Gravimetry of the instantaneous O₂ adsorption

Sample	Degassing temperature/K	Mol ratio en/Co	O ₂ after 1 h/ mols per unit cell
CoY(7.5)	473	5.1	4.7
CoY(13)	473	3.0	8.5
CoY(7.3) ^a	473	2.9	11.2
CoY(1.6) ^b	473	10.0	4.0
CoX(19.5)	473	2.6	23.9
CoA(1.3)	473	3.3	6.7

^a Evacuated at room temperature prior to adsorption of en.
^b Evacuated at 373 K prior to adsorption of en.

bands at 340 and 480 nm found for $[\text{Co}^{\text{III}}(\text{sdmen})\text{Cl}(\text{O}_2)]^+$ (sdmen = *NN'*-dimethylethylenediamine) and interpreted in a similar way.⁴ The shoulder at 500 nm is a *d-d* band of Co^{3+} in the nearly octahedral symmetry of the complex, but it may also represent some unreacted Co^{2+} . The 230 nm band disappears, together with the bands of the mononuclear superoxo-complex, upon room-temperature evacuation. This band represents a $\pi \rightarrow \pi^*$ transition of O_2^- but whether this is an unco-ordinated O_2^- , the O_2^- in the superoxo-complex, or a transient $[\text{Co}(\text{en})(\text{O}_2)]^{2+}$ species analogous to $[\text{Co}(\text{O}_2)\text{L}]^{2+}$ ($\text{L} = 5, 7, 7, 12, 14, 14$ -hexamethyl-1,4,8,11-tetra-azacyclotetra deca-4,11-diene) cannot be decided. The latter absorbs around 230 nm,¹⁴ O_2^- in $\text{K}[\text{O}_2]$ absorbs at 240 nm,¹⁵ and O_2^- in $[\{\text{Co}(\text{CN})_5\}_2(\text{O}_2)]^{5-}$ or in $[\{\text{Co}(\text{NH}_3)_5\}_2(\text{O}_2)]^{5+}$ at 225 nm.¹

The e.s.r. spectrum taken on a similarly pretreated sample (Figure 7) gives unequivocal evidence for a 1:1 superoxo-complex. The spectrum is not the clean O_2^- spectrum of $[\text{Co}(\text{en})_2(\text{O}_2)]^{2+}$.^{7,9} When the decomposition temperature is lowered [Figure 7(b)], the signal of the 1:1 superoxo-

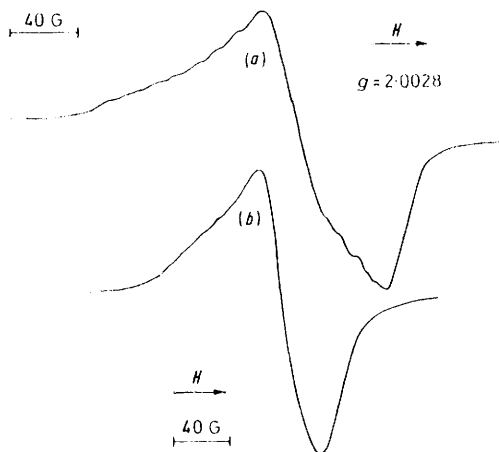


FIGURE 7 E.S.R. spectra of O_2 adducts. (a) Liquid nitrogen spectrum of en-saturated $\text{CoY}(7.1)$, degassed at 505 K, in the presence of O_2 (6.67×10^3 Pa) (7.2×10^3 s contact time). Gain = 1×10^4 . (b) Liquid nitrogen spectrum of en-saturated $\text{CoY}(7.1)$, degassed at 473 ± 3 K, after admission of O_2 (6.67×10^3 Pa) for 300 s and evacuation. Gain = 3.2×10^2 .

complex becomes obscured in a signal with *g* values very close to those of O_2^- .⁷ We suggest that both spectra in Figure 7 are due to a superposition of signals due to the mononuclear superoxo-complex and unco-ordinated O_2^- . The latter predominates at the lower decomposition temperature. It is then tempting to assign the 230 nm band in the reflectance spectrum to unco-ordinated O_2^- . However, whereas the reflectance spectrum of the mononuclear superoxo-complex can be completely eliminated by room-temperature evacuation, this is not the case with its e.s.r. spectrum. We think that this difference is mainly due to the much higher sensitivity of the e.s.r. technique.

What remains in the reflectance spectrum after evacuation of O_2 is a band at 305 nm with a shoulder at 350 nm. Prolonged contact with O_2 intensifies the 305 nm band, the 350 nm band being embedded in its low-frequency tail (Figure 6). This spectrum is identical to that of the monobridged peroxo-complex of Co^{3+} .^{5,16,17} The two bands observed are l.m.c.t. (ligand-to-metal charge-transfer) bands from the split π^* levels of O_2^{2-} to Co^{3+} . However, the 350 nm band may also contain the *d-d* transition of pseudo-

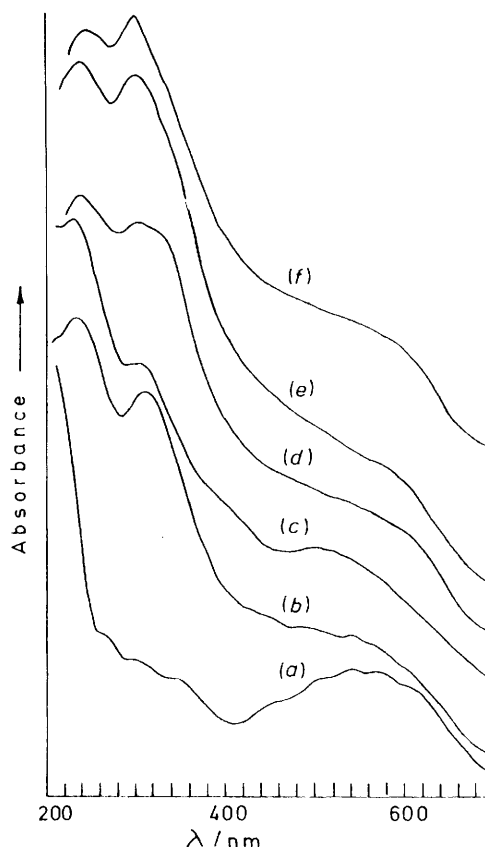


FIGURE 8 Reflectance spectra of the O_2 adducts of $\text{CoY}(17)$ saturated with en. (a) After decomposition at 498 K; (b) immediately after addition of O_2 (6.67×10^3 Pa); (c) after subsequent evacuation overnight; (d) after addition of 50 Torr O_2 [1 Torr = (101 325/760) Pa] for 14.4×10^3 s; (e) after evacuation for 7.2×10^3 s and a 7.2×10^4 s contact with O_2 (6.67×10^3 Pa); (f) after evacuation for 14.4×10^3 s.

octahedral Co^{3+} . The intensity difference between the two l.m.c.t. bands suggests that the $\text{Co}-\text{O}_2^{2-}-\text{Co}$ unit is nearly planar. The in-plane π^* orbital (with σ -bonding character) will give a stronger l.m.c.t. band than the out-of-plane π^* orbital.⁵

The sample $\text{CoY}(17)$, treated in the same temperature range as $\text{CoY}(7.1)$, immediately after admission of O_2 gives [Figure 8(b)] a spectrum with the features of O_2^- (230 nm), the 1:1 superoxo-, and 2:1 monobridged peroxo-complexes and cobalt(II) species. Bands in the range 500–700 nm are characteristic of cobalt(II) species. The simultaneous presence of the two oxygen adducts is shown by the band at 310 nm, in between the characteristic absorptions of the superoxo- (320 nm) and peroxo-complexes (305 nm). It appears that in this case the superoxo-complex : peroxo-complex ratio is lower than for $\text{CoY}(7.1)$. In any case, as for $\text{CoY}(7.1)$, the spectral features of the superoxo-complex are removed by evacuation and the peroxo-complex concentration increases with time of O_2 contact.

As the en degassing temperature is decreased to 473 K and below, an intense O_2^- e.s.r. signal is generated with some 1:1 superoxo-complex superposed on it (Figure 7). The sample has a characteristic pink colour at liquid nitrogen temperature. The reflectance spectra recorded immediately after administration of O_2 shows the 305 nm band of the

peroxo-complex and the 230 nm band of unco-ordinated O_2^- in the case of CoY(17). Figure 9 illustrates that for CoY(7.1) two bands are formed at 305 and at 260 nm. Neither of the bands is removed by evacuation and the

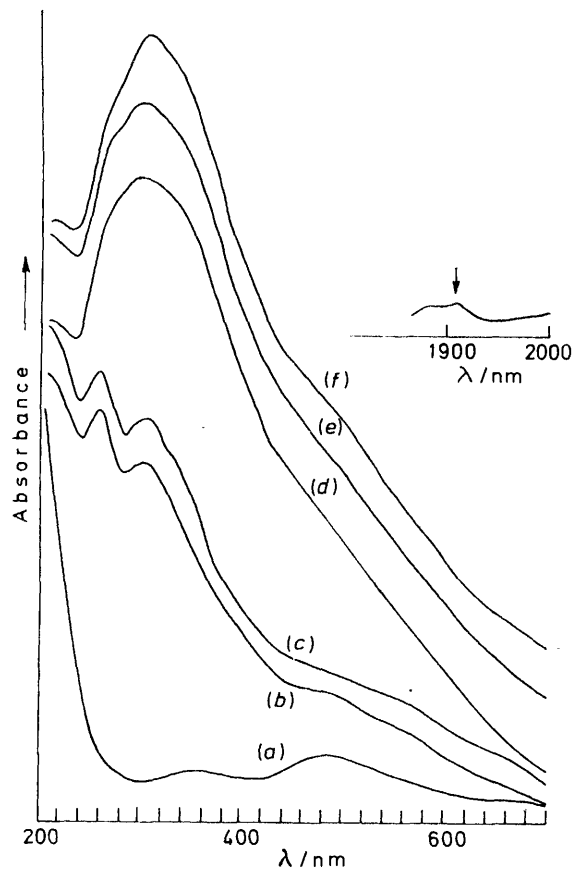


FIGURE 9 Reflectance spectra of O_2 adducts on en-saturated CoY(7.1). (a) After desorption of en at 415 K; (b) immediately after admission of O_2 (6.67×10^3 Pa) at room temperature; (c) after overnight evacuation at room temperature; (d) after a 10.8×10^3 s contact with O_2 (6.67×10^3 Pa) at room temperature; (e) after evacuation over a weekend at room temperature; (f) after contact with O_2 (6.67×10^3 Pa) for 7.2×10^4 s at room temperature

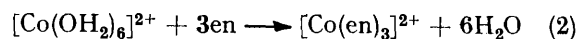
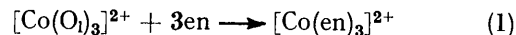
reflectance spectra of both samples become identical after prolonged reaction with O_2 : a 300 nm band with shoulders at ca. 260 nm and ca. 350 nm. Figure 9 also shows that H_2O is formed, characterized by its $\nu + \delta$ vibration at 1910 nm.

DISCUSSION

We have identified by reflectance spectroscopy the mononuclear superoxo-complex $[Co^{III}(en)_2(O_2)]^{2+}$ in the supercages of zeolites Y. Its reflectance spectrum, together with the published e.s.r. spectra and parameters,^{7,9} completes the spectroscopic characterization of the complex. Simultaneously we were able to delineate its formation conditions and to identify other reaction products such as unco-ordinated O_2^- , a mono-bridged peroxodicobalt complex, and water from the oxidation of en. The extent to which each of these reactions occurs depends primarily on the conditions of preparation and on the cobalt(II) content of the zeolites.

Synthesis and Description of $[Co(en)_3]^{2+}$.—Supercage

Co^{2+} , whether hydrated or co-ordinated to lattice oxygens (O_l), reacts instantaneously with gaseous en in a one-step process according to equations (1) and (2).

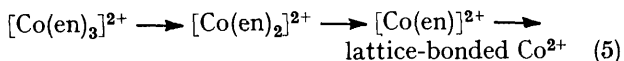
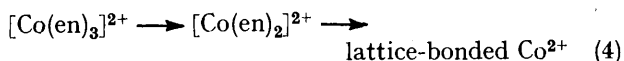
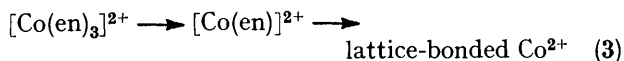


Reaction (2) only involves a replacement of the weaker ligand H_2O by the stronger ligand en in the supercages.

In dehydrated zeolites most of the Co^{2+} , if not all, is located in the hexagonal prisms and cubo-octahedra and is not directly available for co-ordination to en.¹³ The saturation of the supercages with en brings the zeolite into a metastable state and migration of Co^{2+} to the supercages is necessary to obtain a new potential-energy minimum. As soon as Co^{2+} reaches the supercages it co-ordinates to three en molecules because en is a stronger ligand than lattice oxygen atoms. This migration process is very slow at room temperature and depends on the exchangeable cation content. Thus, at low exchange levels, when proportionally more Co^{2+} is in sites I the relative amount of complexed Co^{2+} is low (20%). At high exchange levels appreciable occupation of sites I' and low occupancy of sites II is anticipated and the percentage of Co^{2+} as $[Co(en)_3]^{2+}$ rises to 60% and higher if the small cage sites are made partially inaccessible to Co^{2+} (see Table 2).

We conclude that the migration of Co^{2+} to the supercages is rate determining for complexation in dehydrated cobalt(II) zeolites. Reaction (1) can, however, be completed or nearly so by slow heating up to 423–473 K, because this enhances the mobility of Co^{2+} . The $d-d$ bands of $[Co(en)_3]^{2+}$ are then at 9500 and 19940 cm^{-1} as compared to 10000 and 20650 cm^{-1} in hydrated zeolites. For dehydrated zeolites we calculate¹⁸ $B = 774$ cm^{-1} , $10Dq = 11218$ cm^{-1} and for the hydrated zeolites: $B = 791$ cm^{-1} and $10Dq = 11218$ cm^{-1} . For $[Co(en)_3][NO_3]_2$ Yang and Palmer¹² obtained $B = 810$ cm^{-1} and $10Dq = 11300$ cm^{-1} . There is therefore a small environmental effect on the $[Co(en)_3]^{2+}$ complex.

Decomposition of $[Co(en)_3]^{2+}$.—For the decomposition of the tris complex three possible pathways can be envisaged, equations (3)–(5). A reaction with the



mono complex as intermediate was observed for $[Co(en)_3]-[C_2O_4]$, while a reaction with the bis complex as intermediate was described for $[Co(en)_3]X_2$ ($X = Cl$ or Br).^{19,20}

In zeolites the mono complex is expected to co-ordinate to the lattice, thus making a high-spin pseudo-tetrahedral complex with, typically, two three-component bands in the i.r. and the visible regions.^{21,22} The bis

complex does not directly co-ordinate to lattice oxygens as was shown for the analogous $[\text{Cu}(\text{en})_2]^{2+}$.²³ Thus, there are no axial ligands. Such complexes are low spin and have a $d-d$ spectrum with a characteristic near-i.r. band around $8\,000\text{ cm}^{-1}$ and several $d-d$ bands in the visible region.^{24,25} In the particular case of $[\text{Co}(\text{en})_2][\text{AgI}_2]_2$ two broad bands were reported with maxima at $7\,200\text{ cm}^{-1}$ and $21\,000\text{ cm}^{-1}$.²⁶

Our experimental spectra are not in agreement with the unique presence of bis and mono complexes. The broadening of the $9\,500\text{ cm}^{-1}$ band of $[\text{Co}(\text{en})_3]^{2+}$ towards lower wavenumbers and the appearance of shoulders at $18\,100$ and $22\,000\text{ cm}^{-1}$ may be taken as evidence for the formation of low-spin $[\text{Co}(\text{en})_2]^{2+}$. This is confirmed by a preliminary magnetic susceptibility measurement on $\text{CoY}(5.3)$. The effective magnetic moment of Co^{2+} , uncorrected for the diamagnetism of the zeolite and the adsorbed molecules, was 3.6 B.M.^* after saturation with en and 1.4 B.M. after evacuation at 473 K . However an e.s.r. signal was never detected.²⁷ At present we do not know how to reconcile these contradictory results. The mono complex is unambiguously characterized by reflectance spectroscopy after evacuation at 523 K or above (Figure 4).

Therefore, reaction (5) can be proposed as the decomposition reaction of $[\text{Co}(\text{en})_3]^{2+}$ in the supercages of zeolites on the understanding that the bis complex is a less stable intermediate than the mono complex. In the course of the reaction the conversion of the tris to the bis complex is not yet completed when the decomposition of the bis to the mono complex begins. As a consequence, in the temperature range $470\text{--}510\text{ K}$ a mixture of complexes is present in the supercages. Below 470 K we have $[\text{Co}(\text{en})_3]^{2+}$ and above 510 K $[\text{Co}(\text{en})]^{2+}$.

There is a problem in the spectrum of the mono complexes in that the three u.v. bands ($28\,400$, $32\,600$, and $36\,600\text{ cm}^{-1}$) are difficult to explain. The position of this band system is between the positions of the l.m.c.t. bands of $[\text{CoI}_4]^{2-}$ and $[\text{CoBr}_4]^{2-}$. In these two cases the band system is assigned to $\pi(\text{X}) \rightarrow t_2(\text{Co}^{2+})$ transitions ($\text{X} = \text{I}$ or Br).²⁸ Such filled π orbitals are absent both on lattice oxygens and on en. Dehydrated cobalt(II) zeolites do not have specific u.v. absorptions. It seems, then, that 'en' is necessary to generate this band system. The only explanation, therefore, is the $\sigma(\text{en}) \rightarrow t_2(\text{Co}^{2+})$ charge-transfer transition but this should be confirmed and checked against the other possibilities such as the interaction of Co^{2+} with decomposed en or with lattice defects.

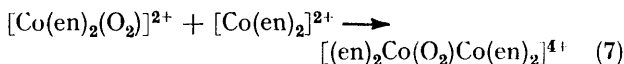
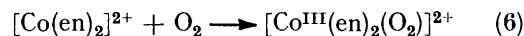
Reactions with O_2 .—Only in the temperature range of decomposition $488\text{--}505\text{ K}$ has it been possible to synthesize detectable amounts of the mononuclear superoxo-complex. Relatively more superoxo-complex is formed on $\text{CoY}(7.1)$ than on $\text{CoY}(17)$. Several conclusions are derived from these observations. (i) The decomposition temperature range in this study lies above that reported by Howe and Lunsford⁷ for maximum superoxo-concen-

tration. This is an illustration of the effect of a difference in amount of material on the desorption processes ($100\text{--}200\text{ mg}$ in e.s.r. cells against $2\text{--}3\text{ g}$ in reflectance cells).

(ii) The ratio mononuclear superoxo-complex: dinuclear, monobridged peroxo-complex is larger at seven Co^{2+} per unit cell than at 17 Co^{2+} per unit cell. Thus, the formation of the peroxo-complex is hindered when, on average, the number of Co^{2+} ions per supercage is less than one. The low mobility of the complexes on the surface is the reason for the stability of the mononuclear superoxo-complex.

(iii) The mononuclear superoxo-complex is not formed on the complexes $[\text{Co}(\text{en})_3]^{2+}$ and $[\text{Co}(\text{en})(\text{O}_1)_3]^{2+}$.

Thus, the reaction leading to the mononuclear superoxo-complex is, as proposed by Howe and Lunsford,⁷ equation (6). The dinuclear monobridged peroxo-complex is then formed according to equation (7).



Reaction (7) is immediate when the supercages contain two cobalt ions $[\text{CoY}(17)]$ but slow when they contain on the average one, or less than one Co^{2+} . In both cases O_2 uptake is immediate as shown in Figure 6. Reactions (6) and (7) are the same as those occurring in solution on cobalt cyanides and $[\text{Co}(\text{sdmen})_2\text{Cl}_2]^{+}$.¹⁷

In the degassing temperature range $410\text{--}473\text{ K}$ $[\text{Co}(\text{en})_3]^{2+}$ is the main species in the supercages. Since there is no free co-ordination site, O_2 must attack the tris complex to form O_2^- immediately. We do not know whether it is in the form of a transient $[\text{Co}(\text{en})_3]^{3+} \cdot \text{O}_2^-$ species or as a free O_2^- ion. In any case, in a slow step en is oxidized with formation of H_2O and an unknown cobalt(III) complex (Figure 9). On $\text{CoY}(17)$ the en:Co ratio is less than $3:1$ (Table 3). This indicates the presence of some bis complex which reacts with O_2 in the initial stages of the reaction to form the peroxo-complex according to (7). This explains the spectral differences between $\text{CoY}(7.1)$ and $\text{CoY}(17)$ in the initial stage of the O_2 interaction.

Description of the $[\text{Co}(\text{en})_2(\text{O}_2)]^{2+}$ Complex.—The spectroscopic data of a series of mononuclear superoxo-complexes with en or its methyl derivative as ligands are summarized in Table 5. There is a very good agreement between the data for our $[\text{Co}(\text{en})_2(\text{O}_2)]^{2+}$ complex and those reported by Pickens *et al.*⁴ In the latter cases the co-ordinated solvent molecule or anion is thought to be *cis* to O_2^- and one N of an sdem molecule *trans* to O_2^- . It is well known that a good σ donor *trans* to O_2^- stabilizes the complex.²⁹

If we formulate our complex in the same way, there is a free co-ordination site *cis* to O_2^- . Otherwise the free co-ordination site is *trans*. In both cases a direct co-ordination of the zeolitic lattice is difficult to imagine. Another factor is the presence of unco-ordinated en especially at low cobalt loading. It may well be that this

* Throughout this paper: $1\text{ B.M.} = 9.274 \times 10^{-24}\text{ A m}^2$.

TABLE 5

Summary of spectroscopic data on mononuclear superoxo-complexes of cobalt

Compound		g_{\parallel}	$A_{\parallel}/\text{cm}^{-1}$	g_{\perp}	A_{\perp}/cm^{-1}	l.m.c.t./nm	Ref.
Cation	Anion						
[Co(sdmen) ₂ (NCMe)(O ₂)] ²⁺	NO ₃ ⁻	2.067	0.002 22	2.008	ca. 0.001 59	308	4
[Co(sdmen) ₂ (NCMe)(O ₂)] ²⁺	Br ⁻	2.068	0.002 12	2.006	ca. 0.001 69	341	4
[Co(sdmen) ₂ (HOMe)(O ₂)] ²⁺	NO ₃ ⁻	2.072	0.002 71	2.009	ca. 0.001 97	327	4
[Co(sdmen) ₂ Cl(O ₂)] ⁺	Cl ⁻	2.075	0.002 52	2.011	ca. 0.001 78	344	4
[Co(en) ₂ (O ₂)] ⁺ -zeolite		2.084	0.001 95	$g_{yy} = 2.007$ $g_{xx} = 1.985$	$A_{yy} = 0.000 97$ $A_{xx} = 0.000 94$	320	This work 9
[Co(CN) ₅ (O ₂)] ³⁻						315-320	3

somehow interacts with the complex at a *trans* position to stabilize the superoxo-complex.

In any case, the e.s.r. parameters are consistent with the formulation Co^{III}-O₂⁻. When the molecular orbital (m.o.) containing the unpaired electron is written as $\psi = \beta|2p\pi_g\rangle + \alpha|3d_{z^2}\rangle$, one calculates the spin density on $3d_{z^2}$ from the anisotropic part of $A_{zz} = A_{\parallel}$ as $\alpha^2 = 0.07-0.10$ for [Co(en)₂(O₂)]²⁺.³⁰ Drago and co-workers³¹ proposed a more complete m.o. [equation (8)].

$$\psi = \alpha'|3d_{z^2}\rangle + \gamma|4s\rangle + \beta|2p\pi_g\rangle \quad (8)$$

A detailed analysis showed that the only source of information of electron transfer from Co to O₂ lies in the spin polarization of the filled Co-O₂ σ bond by the unpaired electron residing in an essentially π^* oxygen m.o. Their analysis of this spin polarization mechanism applied to our [Co(en)₂(O₂)]²⁺ system gives $(\alpha')^2 = 0.24$. The amount of electron transfer from Co to O₂ was calculated to be 0.46 e. The latter value agrees with those calculated by *ab initio* LCAO-MO-SCF methods and by INDO-UHF on [Co(acen)(O₂)] [acen = NN'-ethylenebis(acetylacetonimine)]. In these calculations the amount of electron transfer was in the range 0.44-0.64 e.^{32,33} Although the absolute value of the calculated electron transfer is approximate, the incomplete electron transfer is in agreement with the known X-ray structural data on 1:1 superoxo-complexes.³⁴ The O-O distances ranged between 0.125 and 0.135 nm, as compared with 0.133 nm for O₂⁻ and 0.121 nm for O₂. The lower limit was found with H₂O as axial ligand, the upper limit with pyridine as axial ligand. Thus the amount of electron transfer is dependent on the σ -donor capacity of the ligand *trans* to O₂⁻. The incomplete electron transfer calculated for our [Co(en)₂(O₂)]²⁺ complex indicates that the O-O distance is near the lower limit. This means that a formulation with two en molecules in the plane of the complex and a weakly coordinating surface oxygen or physisorbed en molecule *trans* with respect to O₂⁻ is a reasonable interpretation of our complex.

Conclusions.—Comparing the former e.s.r. work^{7,9} with the present results, one must realize that only the 1:1 superoxo-complex can be detected by e.s.r. while reflectance spectroscopy allows, in principle, the identification of all the cobalt complexes.

Thus, both techniques are complementary and, together with gravimetry, a complete description of the cobalt(II)-en complexes and their O₂ adducts has been made.

1. The migration of Co^{II} to the supercages is rate determining for the formation of [Co(en)₃]²⁺. The same is true for Cu^{II}²³ and reduction of Cu^{II} and Ag^I by H₂ is also limited by the same cationic mobility process.^{35,36}

2. The thermal decomposition *in vacuo* of [Co(en)₃]²⁺ goes through [Co(en)₂]²⁺ and [Co(en)]²⁺. However, the bis complex always occurs in the presence of tris and/or mono complexes. As a consequence, the interaction with O₂ is complicated.

3. The mononuclear superoxocobalt(III) complex is formed instantaneously upon interaction of O₂ with the bis complex on condition that there is, on average, not more than one cobalt atom per supercage. The amount of electron transfer from Co to O₂ is estimated to be 0.46 e. The complex is destroyed by removing O₂ and can only partially be restored.

4. The presence of two cobalt complexes per supercage, either due to a high level of ion exchange or due to migration of complexes accelerated by the presence of physisorbed en, gives rise to dinuclear monobridged peroxocobalt(III) complexes.

5. Oxygen interacts with [Co(en)₃]²⁺ with formation of unidentified cobalt(III) complexes, H₂O, and uncoordinated O₂⁻. Water comes from the oxidation of en but it is not known whether the en is physisorbed or coordinated.

6. Neither dehydrated cobalt(II) nor [Co(en)]²⁺ interacts with O₂.

This work was sponsored by the Belgian Government (Wetenschapsbeleid). One of us (R. A. S.) acknowledges the Belgian 'National Fonds voor Wetenschappelijk Onderzoek' for a grant as 'Onderzoeksleider'. We are indebted to Prof. J. H. Lunsford for many fruitful discussions and to Professors G. Smets and B. Delmon for the use of their e.s.r. machines.

[0/1233 Received, 4th August, 1980]

REFERENCES

- V. M. Miskowski, J. L. Robbins, I. M. Treitel, and H. B. Gray, *Inorg. Chem.*, 1975, **14**, 2318.
- G. McLendon and A. E. Martell, *Coord. Chem. Rev.*, 1976, **19**, 1.
- G. McLendon, S. R. Pickens, and A. E. Martell, *Inorg. Chem.*, 1977, **16**, 1551.
- S. R. Pickens, A. E. Martell, G. McLendon, A. B. P. Lever, and H. B. Gray, *Inorg. Chem.*, 1978, **17**, 2190.
- A. B. P. Lever and H. B. Gray, *Acc. Chem. Res.*, 1978, **11**, 348.
- R. F. Howe and J. H. Lunsford, *J. Am. Chem. Soc.*, 1975, **97**, 5156.
- R. F. Howe and J. H. Lunsford, *J. Phys. Chem.*, 1975, **79**, 1836.
- R. F. Howe and J. H. Lunsford, 'Proceedings of the Sixth

International Congress of Catalysis, The Chemical Society, London, 1976, **1**, 540.

⁹ P. S. E. Dai and J. H. Lunsford, *J. Phys. Chem.*, in the press.

¹⁰ F. Velghe, R. A. Schoonheydt, and J. B. Uytterhoeven, *Clays Clay Miner.*, 1977, **25**, 375.

¹¹ G. Kortüm, 'Reflectance Spectroscopy,' Springer Verlag, Berlin, 1969.

¹² M. C. L. Yang and R. A. Palmer, *J. Am. Chem. Soc.*, 1975, **97**, 5390.

¹³ P. Gallezot and B. Imelik, *J. Chim. Phys. Phys. Biol.*, 1974, **71**, 155.

¹⁴ M. G. Simic and M. Z. Hoffman, *J. Am. Chem. Soc.*, 1977, **99**, 2370.

¹⁵ S. Kim, R. Dicosimo, and J. San Filippo, jun., *Anal. Chem.*, 1979, **51**, 679.

¹⁶ Y. Sasaki, J. Fujita, and K. Saito, *Bull. Chem. Soc. Jpn.*, 1971, **44**, 3373.

¹⁷ S. R. Pickens, Ph.D. Thesis, Texas A & M University, 1978.

¹⁸ E. König, *Struct. Bonding (Berlin)*, 1971, **9**, 175.

¹⁹ J. M. Haschke and W. W. Wendlandt, *Anal. Chim. Acta*, 1974, **8**, 386.

²⁰ L. W. Collins, W. W. Wendlandt, and E. K. Gibson, *Thermochem. Acta*, 1974, **8**, 205.

²¹ F. A. Cotton, D. M. L. Goodgame, and M. Goodgame, *J. Am. Chem. Soc.*, 1961, **83**, 4690.

²² E. R. Menzel, W. R. Vincent, D. K. Johnson, G. L. Seebach, and J. R. Wasson, *Inorg. Chem.*, 1974, **13**, 2465.

²³ P. Peigneur, J. H. Lunsford, W. de Wilde, and R. A. Schoonheydt, *J. Phys. Chem.*, 1977, **81**, 1179.

²⁴ C. J. Hipp and W. A. Baker, jun., *J. Am. Chem. Soc.*, 1970, **92**, 792.

²⁵ F. L. Urbach, R. D. Bereman, J. A. Topich, M. Hariharan, and B. J. Kalbacher, *J. Am. Chem. Soc.*, 1974, **96**, 5063.

²⁶ Y. Nishida and S. Kida, *Bull. Chem. Soc. Jpn.*, 1972, **45**, 461.

²⁷ J. H. Lunsford, personal communication.

²⁸ A. B. P. Lever, 'Inorganic Electronic Spectroscopy,' Elsevier, Amsterdam, 1968, p. 229.

²⁹ M. J. Carter, D. P. Rillema, and F. Basolo, *J. Am. Chem. Soc.*, 1974, **96**, 392.

³⁰ B. M. Hoffman, D. L. Diemente, and F. Basolo, *J. Am. Chem. Soc.*, 1970, **92**, 61.

³¹ B. S. Tovrog, D. J. Kitko, and R. S. Drago, *J. Am. Chem. Soc.*, 1976, **98**, 5144.

³² P. Fantucci and V. Valenti, *J. Am. Chem. Soc.*, 1976, **98**, 3832.

³³ A. Dedieu, M.-M. Rohmer, and A. Veillard, *J. Am. Chem. Soc.*, 1976, **98**, 5789.

³⁴ W. P. Schaefer, B. T. Huie, M. G. Kurilla, and S. E. Ealick, *Inorg. Chem.*, 1980, **19**, 340.

³⁵ H. Beyer, P. A. Jacobs, and J. B. Uytterhoeven, *J. Chem. Soc., Faraday Trans. 1*, 1976, 674.

³⁶ P. A. Jacobs, M. Tielen, J.-P. Linart, and J. B. Uytterhoeven, *J. Chem. Soc., Faraday Trans. 1*, 1976, 2793.